Author Index

Ahmed, M., 37, 127, 135
Anttila, A., 343

Ballhause, P., 399
Bartolucci Luyckx, S., 339
Bennett, M. J., 177
Biederman, R. R., 91
Bishop, H. E., 177
Bodart, F., 111
Budnick, J. I., 149
Budzioch, J., 51
Bunker, S. N., 385

Calliari, L., 349
Carter, G., 21
Cassuto, Y., 339
Chalker, P. R., 177

da Silva, M. R., 161
Dearnaley, G., 191
Deconnick, G., 167
Dillich, S. A., 91, 333
Dimigen, H., 281
Doi, S., 119

Elfenthal, L., 253
Elve, M. A., 13

Färber, R., 327
Fasihuddin, A., 149
Fedrizzi, L., 349
Ferber, H., 213
Fishman, S. G. B., 135
Follstaedt, D. M., 1

Gaiomozzi, F., 197, 349
Gärtner H., 327
Gately, N. V. H., 333
Grant, W. A., 297
Guzman, L., 197, 349

Hale, E. B., 273
Hank, J. G., 317
Hashimoto, S., 119
Hasuyama, H., 9, 33
Hayden, H. C., 149
Hirvonen, J.-P., 13, 343
Hochman, R. F., 317
Hubler, G. K., 243
Hübsch, H., 281

Ingram, D. C., 417
Iwaki, M., 119, 143, 223, 263

Jie, Z., 291
Johnson, H. H., 13

Kanda, Y., 9, 33
Kant, R. A., 357
Katardjiev, I. V., 21
Keller, J. H., 423
Kimura, M., 9, 33
Knapp, J. A., 1
Knystautas, E. J., 173
Kobs, K., 281
Koch, C. H., 149
Kohser, R. A., 273
Koskinen, J., 343
Kossowskiy, R., 307
Kustas, F. M., 407

Laniford, J., 307
Latanision, R. A., 243
Laursen, T., 191
Lefebvre, A., 167
Leitner, K., 253
Lessard, R. A., 173
Leutenecker, R., 281

Madakson, P., 206, 287
Marchetti, F., 197
Margesin, G., 349
Mayer, J. W., 13
McCormick, A. W., 417
Melo, A. A., 161
Meyer, O., 253
Misra, M. S., 407
Molinari, A., 197
Moncoffre, N., 99

Naidu, S. V., 45
Namavar, F., 149
Niiya, K., 9, 33
Nishimura, R., 243
Nobes, M. J., 21

Ohira, S., 143
Ossi, P. M., 55

Paszkeit, C., 343
Pedraza, D. F., 69
Piette, M., 111
Poker, D. B., 417
Potter, D. I., 37, 81, 127, 135
Procter, R. P. M., 297
Pronko, P. P., 417

Reinbold, R., 273
Robinson, J. W., 423
Ruffing, K., 37
Run, L. R., 291
Ryssel, H., 281

Sampath, W. S., 367
Sanchez, F. H., 149
Saqib, M., 81
Saritas, S., 297
Sarkar, M., 197
Sartwell, B. D., 357, 385
Schultze, J. W., 253
Scotoni, M., 349
Sellschop, J. P. F., 339
Sen, P., 45
Singh, A., 173
Sioshansi, P., 373
Smidt, F. A., 385
Snyder, P. G., 417
Soares, J. C., 161
Soeda, T., 33
Soszka, W., 51
Stone, D., 343

Tack, W. T., 407
Takahashi, K., 119
Terasaka, M., 119
Terwagne, G., 111
Thoma, K., 327
Tolle, H. J., 281
Tomasi, A., 197
Tuson, A. T., 177

Vianden, R., 161

Wang, L., 291
Wei, W., 307
Weist, Chr., 399
Weiyi, Y., 291
Whitton, J. L., 21, 191
Wieder, Th, 327
Wilbur, P. H., 367
Wolf, G. K. 213, 237, 399
Wollam, J. A., 417

Yawen, S., 291

0025-5416/87/$3.50

© Elsevier Sequoia/Printed in The Netherlands

Subject Index

Adiabatic engines
  friction and wear of ion-beam-modified ceramics for use in high temperature adiabatic engines, 307
Alloys
  effect of nitrogen and boron ion on cyclic deformation response in Ti–24V alloy, 317
  electrochemical properties of chromium-implanted Fe–Cr alloys, 223
  structural changes in a cobalt-based alloy after high fluence ion implantation, 91
  use of ion implantation to modify the tribological properties of Ti–6Al–4V alloy, 297
Aluminium
  amorphous phase formation in aluminum-ion-implanted refractory metals, 81
  characterization of the aluminium surface layer implanted with nitrogen, 143
  compositional instabilities in aluminum-implanted nickel, 127
  effect of temperature on high fluence transition metal implants into polycrystalline aluminum, 149
  formation of icosahedral Al–Mn and Al–Ru by solid state processes, 1
  use of ion implantation to modify the tribological properties of Ti–6Al–4V alloy, 297
Amorphization
  amorphization of intermetallic compounds by ion bombardment, 69
  ion-beam-induced amorphization, 55
Amorphous phase formation
  amorphous phase formation in aluminum-ion-implanted refractory metals, 81
Argon
  hydrogen permeation behavior in polycrystalline nickel implanted with helium, argon, nickel, yttrium and platinum, 243
Aqueous corrosion
  aqueous corrosion behaviour of ion-implanted metals, 213

Bearing steel
  mechanical properties of nitrogen-implanted 18W–4Cr–1V bearing steel, 287
Beryllium
  improvement in the wear properties of GCr15–QBe2 wear pairs by ion implantation, 291
Boron
  effect of nitrogen and boron ion on cyclic deformation response in Ti–24V alloy, 317
  oxidation inhibition of iron by deposited and ion-implanted boron, 197
  quantitative analysis of boron in steel by secondary ion mass spectrometry using ion-implanted iron as standard, 119
Boron nitride
  characterization of ion-beam-synthesized boron nitride films, 173

Carbon
  characterization of ion-beam-induced carbon deposition on WC–Co hard metal by microhardness, scratch and abrasive wear tests, 343
Carbon dioxide
  influence of cerium, yttrium and lanthanum ion implantation on the oxidation behaviour of a 20Cr–25Ni–Nb stainless steel in carbon dioxide at 900–1050 °C, 177
Cavitation erosion
  effects of titanium implantation on cavitation erosion of cobalt-based metal–carbide systems, 333
Ceramics
  friction and wear of ion-beam-modified ceramics for use in high temperature adiabatic engines, 307
Cerium
  influence of cerium, yttrium and lanthanum ion implantation on the oxidation behaviour of a 20Cr–25Ni–Nb stainless steel in carbon dioxide at 900–1050 °C, 177
Chromium
  electrochemical properties of chromium-implanted Fe–Cr alloys, 223
  improvement in the wear properties of GCr15–QBe2 wear pairs by ion implantation, 291
  influence of cerium, yttrium and lanthanum ion implantation on the oxidation behaviour of a 20Cr–25Ni–Nb stainless steel in carbon dioxide at 900–1050 °C, 177
  mechanical properties of nitrogen-implanted 18W–4Cr–1V bearing steel, 287
  surface modification of electrodeposited chromium films by ion implantation, 229
Cobalt
  characterization of ion-beam-induced carbon deposition on WC–Co hard metal by microhardness, scratch and abrasive wear tests, 343
  effects of titanium implantation on cavitation erosion of cobalt-based metal–carbide systems, 333
  structural changes in a cobalt-based alloy after high fluence ion implantation, 91
Compositional instabilities
  compositional instabilities in aluminum-implanted nickel, 127
Cone-shaped thin wires
  ion-beam-induced morphological evolution of cone-shaped thin wires, 33
Critical angle of incidence
  measurements of sputtering yield at the critical angle of incidence, 9

0025-5416/87/$3.50

© Elsevier Sequoia/Printed in The Netherlands

Cyclic deformation
effect of nitrogen and boron ion on cyclic deformation response in Ti–24V alloy, 317

Deposition
characterization of ion-beam-induced carbon deposition on WC–Co hard metal by microhardness, scratch and abrasive wear tests, 343
thick and homogeneous surface layers obtained by reactive ion-beam-enhanced deposition, 349
Depth profiling
migration studies of nitrogen-implanted-iron by improved depth profiling, 111
Ductile-to-brittle transition
ductile-to-brittle transition induced by nitrogen ion implantation into WC single crystals, 339

Electrochemical
electrochemical properties of chromium-implanted Fe–Cr alloys, 223
electrochemical studies of TiO_2 films with various palladium implantation profiles, 253
Electrodeposited chromium films
surface modification of electrodeposited chromium films by ion implantation, 229

Fatigue
structure and fatigue properties of ion-plated nickel films on steel, 327
Fatigue resistance
nitrogen implantation of type 303 stainless steel gears for improved wear and fatigue resistance, 407
Films
characterization of ion-beam-synthesized boron nitride films, 173
electrochemical studies of TiO_2 films with various palladium implantation profiles, 253
Friction
friction and wear of ion-beam-modified ceramics for use in high temperature adiabatic engines, 307

Gears
nitrogen implantation of type 303 stainlesss steel gears for improved wear and fatigue resistance, 407
Gold
study of gold-implanted magnesium metastable system, 161

Hard metal
characterization of ion-beam-induced carbon deposition on WC–Co hard metal by microhardness, scratch and abrasive wear tests, 343
Helium
hydrogen permeation behavior in polycrystalline nickel implanted with helium, argon, nickel, yttrium and platinum, 243
High energy α-bombarded molybdenum surfaces
scanning electron microscopy observation of high energy α-bombarded molybdenum surfaces, 45
High temperature adiabatic engines
friction and wear of ion-beam-modified ceramics for use in high temperature adiabatic engines, 307
Hydrogen embrittlement
influence of platinum implantation on the hydrogen embrittlement of tantalum, 237
Hydrogen permeation
hydrogen permeation behavior in polycrystalline nickel implanted with helium, argon, nickel, yttrium and platinum 243
Hydrogenated multilayer Fe–Ti and Ni–Ti films
ion beam mixing of hydrogenated multilayer Fe–Ti and Ni–Ti films, 13

Icosahedral
formation of icosahedral Al–Mn and Al–Ru by solid state processes, 1
Implantation
nitrogen implantation into steels, 99
surface roughening during elevated temperature implantation of nickel, 37
Implantation profiles
electrochemical studies of TiO_2 films with various palladium implantation profiles, 253
Implantation systems
ion sources and implantation systems, 423
Industrial components
surface modification of industrial components by ion implantation, 373
Intermetallic compounds
amorphization of intermetallic compounds by ion bombardment, 69
Ion beams
new rapid technique for characterizing microstructures of films produced by ion beams in the transmission electron microscope, 367
Ion-beam-induced amorphization
ion-beam-induced amorphization, 55
Ion beam mixing
enhanced endurance life of sputtered MoS_x films on steel by ion beam mixing, 281
ion beam mixing of hydrogenated multilayer Fe–Ti and Ni–Ti films, 13
Ion beam modification
ion beam modification of TiN films during vapor deposition, 357
Ion-beam-modified ceramics
friction and wear of ion-beam-modified ceramics for use in high temperature adiabatic engines, 307
Ion beam smoothing
ion beam smoothing of metallic mirrors, 417
Ion-beam-synthesized boron nitride films
characterization of ion-beam-synthesized boron nitride films 173
Ion bombardment
amorphization of intermetallic compounds by ion bombardment, 69
surface texture induced by heavy ion bombardment: ion reflection analysis, 51
Ion implantation
ductile-to-brittle transition induced by nitrogen ion implantation into WC single crystals, 339

effects of tin ion and nitrogen ion implantation on the oxidation of titanium, 205
improvement in the wear properties of GCr15-QBe2 wear pairs by ion implantation, 291
improving the wear resistance of metal-forming tools by ion implantation, 399
influence of cerium, yttrium and lanthanum ion implantation on the oxidation behaviour of a 20Cr-25Ni-Nb stainless steel in carbon dioxide at 900-1050 °C, 177
structural changes in a cobalt-based alloy after high fluence ion implantation, 91
surface modification of electrodeposited chromium films by ion implantation, 229
surface modification of industrial components by ion implantation, 373
U.S. Navy Manufacturing Technology Program on ion implantation, 385
use of ion implantation to modify the tribological properties of Ti-6Al-4V alloy, 297
Ion-implanted metals
aqueous corrosion behaviour of ion-implanted metals, 213
Ion mass spectrometry
quantitative analysis of boron in steel by secondary ion mass spectrometry using ion-implanted iron as standard, 119
Ion-plated nickel films
structure and fatigue properties of ion-plated nickel films on steel, 327
Ion reflection analysis
surface texture induced by heavy ion bombardment: ion reflection analysis, 51
Ion sources
ion sources and implantation systems, 423
Iron
electrochemical properties of chromium-implanted Fe-Cr alloys, 223
ion beam mixing of hydrogenated multilayer Fe-Ti and Ni-Ti films, 13
migration studies of nitrogen-implanted-iron by improved depth profiling, 111
oxidation inhibition of iron by deposited and ion-implanted boron, 197
quantitative analysis of boron in steel by secondary ion mass spectrometry using ion-implanted iron as standard, 119

Lanthanum
influence of cerium, yttrium and lanthanum ion implantation on the oxidation behaviour of a 20Cr-25Ni-Nb stainless steel in carbon dioxide at 900-1050 °C, 177

Magnesium
study of gold-implanted magnesium metastable system, 161
Manganese
formation of icosahedral Al-Mn and Al-Ru by solid state processes, 1
Mechanical properties
mechanical properties of nitrogen-implanted 18W-4Cr-1V bearing steel, 287
Metal-carbide
effects of titanium implantation on cavitation erosion of cobalt-based metal-carbide systems, 333
Metal-forming tools
improving the wear resistance of metal-forming tools by ion implantation, 399
Metallic mirrors
ion beam smoothing of metallic mirrors, 417
Metals
amorphous phase formation in aluminum-ion-implanted refractory metals, 81
aqueous corrosion behaviour of ion-implanted metals, 213
induced X-ray emission from neon implanted into metals, 167
sputtering-induced surface topography on F.C.C. metals, 21
Metastable system
study of gold-implanted magnesium metastable system, 161
Microhardness
characterization of ion-beam-induced carbon deposition on WC-Co hard metal by microhardness, scratch and abrasive wear tests, 343
Microstructures
compounds and microstructures of silicon implanted nickel, 135
new rapid technique for characterizing microstructures of films produced by ion beams in the transmission electron microscope, 367
Migration
migration studies of nitrogen-implanted-iron by improved depth profiling, 111
Mirrors
ion beam smoothing of metallic mirrors, 417
Molybdenum
scanning electron microscopy observation of high energy α-bombarded molybdenum surfaces, 45
Molybdenum sulphide
enhanced endurance life of sputtered MoS_x films on steel by ion beam mixing, 281
Morphological
ion-beam-induced morphological evolution of cone-shaped thin wires, 33

Neon
induced X-ray emission from neon implanted into metals, 167
Nickel
compositional instabilities in aluminum-implanted nickel, 127
compounds and microstructures of silicon implanted nickel, 135
hydrogen permeation behavior in polycrystalline nickel implanted with helium, argon, nickel, yttrium and platinum, 243
influence of cerium, yttrium and lanthanum ion implantation on the oxidation behaviour of a 20Cr-25Ni-Nb stainless steel in carbon dioxide at 900-1050 °C, 177
ion beam mixing of hydrogenated multilayer Fe-Ti and Ni-Ti films, 13
structure and fatigue properties of ion-plated nickel films on steel, 327

surface roughening during elevated temperature implantation of nickel, 37
Niobium
influence of cerium, yttrium and lanthanum ion implantation on the oxidation behaviour of a 20Cr–25Ni–Nb stainless steel in carbon dioxide at 900–1050 °C, 177
Nitrogen
characterization of the aluminium surface layer implanted with nitrogen, 143
ductile-to-brittle transition induced by nitrogen ion implantation into WC single crystals, 339
effect of nitrogen and boron ion on cyclic deformation response in Ti–24V alloy, 317
effects of tin ion and nitrogen ion implantation on the oxidation of titanium, 205
mechanical properties of nitrogen-implanted 18W–4Cr–1V bearing steel, 287
migration studies of nitrogen-implanted-iron by improved depth profiling, 111
nitrogen implantation of steels: a treatment which can initiate sustained oxidative wear, 273
nitrogen implantation of type 303 stainless steel gears for improved wear and fatigue resistance, 407
Nitrogen implantation
nitrogen implantation into steels, 99

Oxidation
effects of tin ion and nitrogen ion implantation on the oxidation of titanium, 205
the influence of cerium, yttrium and lanthanum ion implantation on the oxidation behaviour of a 20Cr–25Ni–Nb stainless steel in carbon dioxide at 900–1050 °C, 177
oxidation inhibition of iron by deposited and ion-implanted boron, 197
Rutherford backscattering-channelling study of yttrium-implanted stainless steel before and after oxidation, 191
Oxidative wear
nitrogen implantation of steels: a treatment which can initiate sustained oxidative wear, 273

Palladium
electrochemical studies of TiO_2 films with various palladium implantation profiles, 253
Platinum
hydrogen permeation behavior in polycrystalline nickel implanted with helium, argon nickel, yttrium and platinum, 243
influence of platinum implantation on the hydrogen embrittlement of tantalum, 237

Reactive ion-beam-enhanced deposition
thick and homogeneous surface layers obtained by reactive ion-beam-enhanced deposition, 349
Ruthenium
formation of icosahedral Al–Mn and Al–Ru by solid state processes, 1
Rutherford backscattering-channelling study
Rutherford backscattering-channelling study of yttrium-implanted stainless steel before and after oxidation, 191

Scanning electron microscopy
scanning electron microscopy observation of high energy α-bombarded molybdenum surfaces, 45
Silicon
compounds and microstructures of silicon implanted nickel, 135
Solid state processes
formation of icosahedral Al–Mn and Al–Ru by solid state processes, 1
Sputtering
sputtering-induced surface topography on F.C.C. metals, 21
Sputtered MoS_x films
enhanced endurance life of sputtered MoS_x films on steel by ion beam mixing, 281
Sputtering yield
measurements of sputtering yield at the critical angle of incidence, 9
Stainless steel
influence of cerium, yttrium and lanthanum ion implantation on the oxidation behaviour of a 20Cr–25Ni–Nb stainless steel in carbon dioxide at 900–1050 °C, 177
nitrogen implantation of type 303 stainless steel gears for improved wear and fatigue resistance, 407
Stainless steel
Rutherford backscattering-channelling study of yttrium-implanted stainless steel before and after oxidation, 191
Steels
enhanced endurance life of sputtered MoS_x films on steel by ion beam mixing, 281
mechanical properties of nitrogen-implanted 18W–4Cr–1V bearing steel, 287
nitrogen implantation into steels, 99
nitrogen implantation of steels: a treatment which can initiate sustained oxidative wear, 273
quantitative analysis of boron in steel by secondary ion mass spectrometry using ion-implanted iron as standard, 119
structure and fatigue properties of ion-plated nickel films on steel, 327
tribological properties of ion-implanted steels, 263
Surface
surface roughening during elevated temperature implantation of nickel, 37
surface texture induced by heavy ion bombardment: ion reflection analysis, 51
Surface modification
surface modification of electrodeposited chromium films by ion implantation, 229
surface modification of industrial components by ion implantation, 373
Surface topography
sputtering-induced surface topography on F.C.C. metals, 21

Tantalum
influence of platinum implantation on the hydrogen embrittlement of tantalum, 237
Tin
effects of tin ion and nitrogen ion implantation on the oxidation of titanium, 205

Titanium
effect of nitrogen and boron ion on cyclic deformation response in Ti–24V alloy, 317
effects of tin ion and nitrogen ion implantation on the oxidation of titanium, 205
effects of titanium implantation on cavitation erosion of cobalt-based metal–carbide systems, 333
ion beam mixing of hydrogenated multilayer Fe–Ti and Ni–Ti films, 13
use of ion implantation to modify the tribological properties of Ti–6Al–4V alloy, 297
Titanium nitride
ion beam modification of TiN films during vapor deposition, 357
Titanium oxide
electrochemical studies of TiO_2 films with various palladium implantation profiles, 253
Transition metal
effect of temperature on high fluence transition metal implants into polycrystalline aluminum, 149
Transmission electron microscope
new rapid technique for characterizing microstructures of films produced by ion beams in the transmission electron microscope, 367
Tribological properties
tribological properties of ion-implanted steels, 263
use of ion implantation to modify the tribological properties of Ti–6Al–4V alloy, 297
Tungsten
mechanical properties of nitrogen-implanted 18W–4Cr–1V bearing steel, 287
Tungsten carbide
characterization of ion-beam-induced carbon deposition on WC–Co hard metal by microhardness, scratch and abrasive wear tests, 343
ductile-to-brittle transition induced by nitrogen ion implantation into WC single crystals, 339

Vanadium
effect of nitrogen and boron ion on cyclic deformation response in Ti–24V alloys, 317
mechanical properties of nitrogen-implanted 18W–4Cr–1V bearing steel, 287
use of ion implantation to modify the tribological properties of Ti–6Al–4V alloy, 297
Vapour deposition
ion beam modification of TiN films during vapor deposition, 357

Wear
characterization of ion-beam-induced carbon deposition on WC–Co hard metal by microhardness, scratch and abrasive wear tests, 343
friction and wear of ion-beam-modified ceramics for use in high temperature adiabatic engines, 307
improvement in the wear properties of GCr15–QBe2 wear pairs by ion implantation, 291
improving the wear resistance of metal-forming tools by ion implantation, 399
nitrogen implantation of steels: a treatment which can initiate sustained oxidative wear, 273
nitrógen implantation of type 303 stainless steel gears for improved wear and fatigue resistance, 407
WC single crystals
ductile-to-brittle transition induced by nitrogen ion implantation into WC single crystals, 339

X-ray emission
induced X-ray emission from neon implanted into metals, 167

Yttrium
influence of cerium, yttrium and lanthanum ion implantation on the oxidation behaviour of a 20Cr–25Ni–Nb stainless steel in carbon dioxide at 900–1050 °C, 177
Rutherford backscattering-channelling study of yttrium-implanted stainless steel before and after oxidation, 191
hydrogen permeation behavior in polycrystalline nickel implanted with helium, argon, nickel, yttrium and platinum, 243

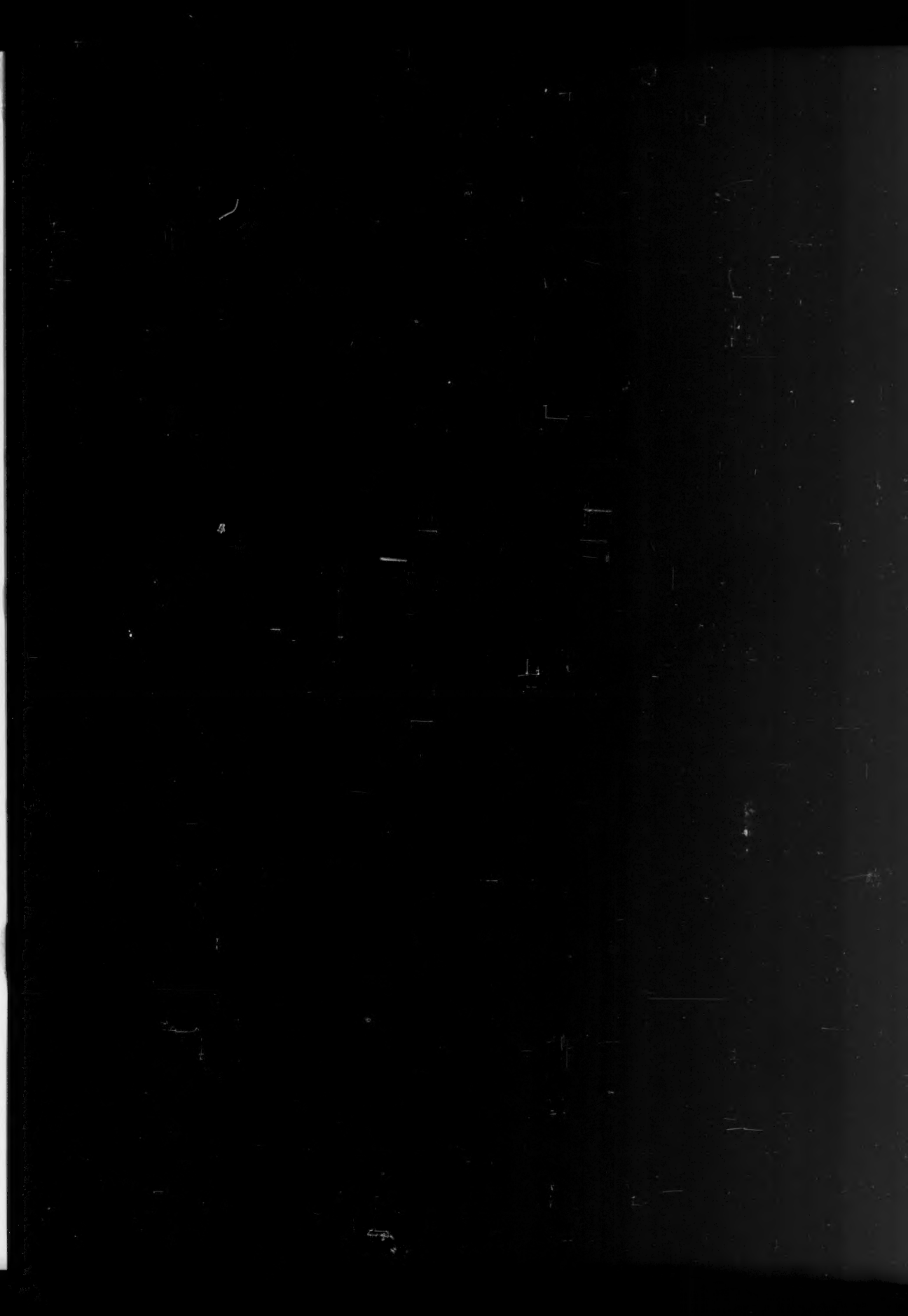

CONTENTS

Preface v
Conference organization vi

FUNDAMENTAL ASPECTS

Formation of icosahedral Al–Mn and Al–Ru by solid state processes 1
D. M. Follstaedt and J. A. Knapp (Albuquerque, NM, U.S.A.)

Measurements of sputtering yield at the critical angle of incidence 9
H. Hasuyama, Y. Kanda, K. Niiya and M. Kimura (Fukuoka, Japan)

Ion beam mixing of hydrogenated multilayer Fe–Ti and Ni–Ti films 13
J.-P. Hirvonen, M. A. Elve, J. W. Mayer and H. H. Johnson (Ithaca, NY, U.S.A.)

SURFACE MORPHOLOGY

Sputtering-induced surface topography on F.C.C. metals. 21
G. Carter, I. V. Katardjiev, M. J. Nobes (Salford, U.K.) and J. L. Whitton (Kingston, Ontario, Canada)

Ion-beam-induced morphological evolution of cone-shaped thin wires 33
H. Hasuyama, K. Kanda, T. Soeda, K. Niiya and M. Kimura (Fukuoka, Japan)

Surface roughening during elevated temperature implantation of nickel 37
M. Ahmed, K. Ruffing and D. I. Potter (Storrs, CT, U.S.A.)

Scanning electron microscopy observation of high energy α-bombarded molybdenum surfaces. 45
S. V. Naidu and P. Sen (Calcutta, India)

Surface texture induced by heavy ion bombardment: ion reflection analysis. 51
J. Budzioch and W. Soszka (Krakow, Poland)

AMORPHIZATION

Ion-beam-induced amorphization 55
P. M. Ossi (Milan, Italy)

Amorphization of intermetallic compounds by ion bombardment. 69
D. F. Pedraza (Oak Ridge, TN, U.S.A.)

Amorphous phase formation in aluminum-ion-implanted refractory metals. 81
M. Saqib and D. I. Potter (Storrs, CT, U.S.A.)

Structural changes in a cobalt-based alloy after high fluence ion implantation 91
S. A. Dillich and R. R. Biederman (Worcester, MA, U.S.A.)

CHARACTERIZATION

Nitrogen implantation into steels 99
N. Moncoffre (Villeurbanne, France)

Migration studies of nitrogen-implanted-iron by improved depth profiling 111
F. Bodart, G. Terwagne and M. Piette (Namur, Belgium)

Quantitative analysis of boron in steel by secondary ion mass spectrometry using ion-implanted iron as standard 119
S. Hashimoto, S. Doi, K. Takahashi, M. Terasaka (Kanagawa, Japan) and M. Iwaki (Saitama, Japan)

Compositional instabilities in aluminum-implanted nickel 127
M. Ahmed and D. I. Potter (Storrs, CT, U.S.A.)

Compounds and microstructures of silicon-implanted nickel 135
S. G. B. Fishman, M. Ahmed and D. I. Potter (Storrs, CT, U.S.A.)

Characterization of the aluminium surface layer implanted with nitrogen. 143
S. Ohira (Shizuoka-ken, Japan) and M. Iwaki (Saitama-ken, Japan)

Effect of temperature on high fluence transition metal implants into polycrystalline aluminum 149
F. H. Sanchez, F. Namavar, J. I. Budnick, A. Fasihuddin, C. H. Koch and H. C. Hayden (Storrs, CT, U.S.A.)

Study of a gold-implanted magnesium metastable system 161
M. R. da Silva, A. A. Melo, J. C. Soares (Lisbon, Portugal), M. F. da Silva (Sacavém, Portugal) and R. Vianden (Bonn, F.R.G.)

Induced X-ray emission from neon implanted into metals 167
G. Deconninck and A. Lefebvre (Namur, Belgium)

Characterization of ion-beam-synthesized boron nitride films. 173
A. Singh, R. A. Lessard and E. J. Knystautas (Quebec, Canada)

OXIDATION

The influence of cerium, yttrium and lanthanum ion implantation on the oxidation behaviour of a 20Cr–25Ni–Nb stainless steel in carbon dioxide at 900–1050 °C 177
M. J. Bennett, H. E. Bishop, P. R. Chalker and A. T. Tuson (Didcot, U.K.)

A Rutherford backscattering-channelling study of yttrium-implanted stainless steel before and after oxidation. 191
G. Dearnaley (Didcot, U.K.), T. Laursen and J. L. Whitton (Kingston, Ontario, Canada)

Oxidation inhibition of iron by deposited and ion-implanted boron 197
F. Giacomozzi, L. Guzman, F. Marchetti, A. Molinari, M. Sarkar and A. Tomasi (Povo, Italy)

Effects of tin ion and nitrogen ion implantation on the oxidation of titanium. 205
P. Madakson (Yorktown Heights, NY, U.S.A.)

CORROSION

Aqueous corrosion behaviour of ion-implanted metals 213
H. Ferber and G. K. Wolf (Heidelberg, F.R.G.)

Electrochemical properties of chromium-implanted Fe–Cr alloys 223
Y. Okabe, M. Iwaki and K. Takahashi (Saitama, Japan)

Surface modification of electrodeposited chromium films by ion implantation 229
K. Terashima, T. Minegishi (Chiba, Japan), M. Iwaki (Saitama, Japan) and K. Kawashima (Tokyo, Japan)

The influence of platinum implantation on the hydrogen embrittlement of tantalum 237
W. Ensinger and G. K. Wolf (Heidelberg, F.R.G.)

Hydrogen permeation behavior in polycrystalline nickel implanted with helium, argon, nickel, yttrium and platinum 243
R. Nishimura, R. M. Latanision (Cambridge, MA, U.S.A.) and G. K. Hubler (Washington, DC, U.S.A.)

Electrochemical studies of TiO_2 films with various palladium implantation profiles 253
J. W. Schultze, L. Elfenthal, K. Leitner (Düsseldorf, F.R.G.) and O. Meyer (Karlsruhe, F.R.G.)

WEAR

Tribological properties of ion-implanted steels 263
M. Iwaki (Saitama, Japan)

Nitrogen implantation of steels: a treatment which can initiate sustained oxidative wear. 273
E. B. Hale, R. Reinbold and R. A. Kohser (Rolla, MO, U.S.A.)

Enhanced endurance life of sputtered MoS_x films on steel by ion beam mixing 281
K. Kobs, H. Dimigen, H. Hübsch, H. J. Tolle (Hamburg, F.R.G.), R. Leutenecker (München, F.R.G.) and H. Ryssel (Erlangen, F.R.G.)

Mechanical properties of nitrogen-implanted 18W–4Cr–1V bearing steel. 287
P. Madakson (Yorktown Heights, NY, U.S.A.)

The improvement in the wear properties of GCr15–QBe2 wear pairs by ion implantation 291
Z. Jie, S. Yawen, L. Guanguan, L. F. Run, Y. Weiyi and L. Wang (Tianjin, China)

The use of ion implantation to modify the tribological properties of Ti–6Al–4V alloy 297
S. Saritas (Gaziantep, Turkey), R. P. M. Procter (Manchester, U.K.) and W. A. Grant (Salford, U.K.)

Friction and wear of ion-beam-modified ceramics for use in high temperature adiabatic engines 307
W. Wei, J. Lankford (San Antonio, TX, U.S.A.) and R. Kossowsky (University Park, PA, U.S.A.)

MECHANICAL PROPERTIES

The effect of nitrogen and boron ion on cyclic deformation response in Ti–24V alloy 317
J. G. Han and R. F. Hochman (Atlanta, GA, U.S.A.)

Structure and fatigue properties of ion-plated nickel films on steel 327
K. Thoma, R. Färber, Th. Wieder and H. Gärtner (Kassel, F.R.G.)

Effects of titanium implantation on cavitation erosion of cobalt-based metal–carbide systems 333
N. V. H. Gately and S. A. Dillich (Worcester, MA, U.S.A.)

Ductile-to-brittle transition induced by nitrogen ion implantation into WC single crystals 339
S. Bartolucci Luyckx, Y. Cassuto and J. P. F. Sellschop (Johannesburg, South Africa)

Characterization of ion-beam-induced carbon deposition on WC–Co hard metal by microhardness, scratch and abrasive wear tests 343
J.-P. Hirvonen, J. Koskinen, A. Anttila (Helsinki, Finland), D. Stone and C. Paszkiet (Ithaca, NY, U.S.A.)

NOVEL TECHNIQUES

Thick and homogeneous surface layers obtained by reactive ion-beam-enhanced deposition 349
L. Guzman, F. Giacomozzi, B. Margesin, L. Calliari, L. Fedrizzi, P. M. Ossi (Povo, Italy) and M. Scotoni (Trento, Italy)

Ion beam modification of TiN films during vapor deposition 357
R. A. Kant and B. D. Sartwell (Washington, DC, U.S.A.)

A new rapid technique for characterizing microstructures of films produced by ion beams in the transmission electron microscope 367
W. S. Sampath and P. J. Wilbur (Fort Collins, CO, U.S.A.)

APPLICATIONS

Surface modification of industrial components by ion implantation 373
P. Sioshansi (Bedford, MA, U.S.A.)

U.S. Navy Manufacturing Technology Program on ion implantation 385
F. A. Smidt, B. D. Sartwell (Washington, DC, U.S.A.) and S. N. Bunker (Bedford, MA, U.S.A.)

Improving the wear resistance of metal-forming tools by ion implantation 399
Chr. Weist, G. K. Wolf (Stuttgart, F.R.G.) and P. Ballhause (Heidelberg, F.R.G.)

Nitrogen implantation of type 303 stainless steel gears for improved wear and fatigue resistance 407
F. M. Kustas, M. S. Misra and W. T. Tack (Denver, CO, U.S.A.)

Ion beam smoothing of metallic mirrors 417
D. C. Ingram, A. W. McCormick, P. P. Pronko (Dayton, OH, U.S.A.), J. A. Woollam, P. G. Snyder (Lincoln, NE, U.S.A.) and D. B. Poker (Oak Ridge, TN, U.S.A.)

Ion sources and implantation systems 423
J. H. Keller (Hopewell Junction, NY, U.S.A.) and J. W. Robinson (University Park, PA, U.S.A.)

AUTHOR INDEX 433

SUBJECT INDEX 434